



Molecular Crystals and Liquid Crystals Science and Technology. Section A. Molecular Crystals and Liquid Crystals

Publication details, including instructions for authors and
subscription information:

<http://www.tandfonline.com/loi/gmcl19>

Exceptional Dispersion in DNP Crystals in the Visible Spectral Range

Hans W. Helberg^a & Andrea Bank^a

^a Drittes Physikalisches Institut, Universität Göttingen, Germany
Version of record first published: 24 Sep 2006.

To cite this article: Hans W. Helberg & Andrea Bank (1994): Exceptional Dispersion in DNP Crystals in the Visible Spectral Range, *Molecular Crystals and Liquid Crystals Science and Technology. Section A. Molecular Crystals and Liquid Crystals*, 252:1, 175-183

To link to this article: <http://dx.doi.org/10.1080/10587259408038223>

PLEASE SCROLL DOWN FOR ARTICLE

Full terms and conditions of use: <http://www.tandfonline.com/page/terms-and-conditions>

This article may be used for research, teaching, and private study purposes. Any substantial or systematic reproduction, redistribution, reselling, loan, sub-licensing, systematic supply, or distribution in any form to anyone is expressly forbidden.

The publisher does not give any warranty express or implied or make any representation that the contents will be complete or accurate or up to date. The accuracy of any instructions, formulae, and drug doses should be independently verified with primary sources. The publisher shall not be liable for any loss, actions, claims, proceedings, demand, or costs or damages whatsoever or howsoever caused arising directly or indirectly in connection with or arising out of the use of this material.

EXCEPTIONAL DISPERSION IN DNP CRYSTALS IN THE VISIBLE SPECTRAL RANGE

HANS W. HELBERG and ANDREA BANK

Drittes Physikalisches Institut, Universität Göttingen, Germany

Abstract In DNP monomer crystals the indicatrix, the optic axes angle, the birefringence, and the absorption tensor were measured in the VIS and NIR spectral range. A crossed-axial-plane dispersion is found with change of the plane orientation in the green region ($1.9 \cdot 10^4 \text{ cm}^{-1}$) of the spectrum. Calculations of the polarizability tensor by tensorial addition of the bond polarizabilities show that the polarizabilities of the molecules only can not yield the measured orientation of the indicatrix. Polarizabilities with other orientations must be involved. Assigning polarizabilities to intermolecular contacts with short distances can explain the measured behavior.

Keywords: dispersion, DNP, ferroelectric, birefringence, polarizability

INTRODUCTION

The disubstituted diacetylene 1,6-bis(2,4-dinitrophenoxy)-2,4-hexadiyne (DNP) belongs to molecules of the kind $\text{R}-\text{C}\equiv\text{C}-\text{C}\equiv\text{C}-\text{R}$.^{1,2} Crystals from these molecules show very interesting properties.^{1,2} Annealing or treatment with UV or X rays of these crystals initiates polymerization and forms conjugate chains. The polymer crystals are of high perfection.

Especially the dielectric properties of monomer crystals of DNP were investigated.^{3,4} DNP undergoes a ferroelectric phase transition at 46 K mainly due to the loss of the centrosymmetry of the molecules by twisting of the two aromatic groups by about 50° .^{5,6}

In connection with our investigations of the microwave dielectric properties⁷ we also looked through the crystals with polarized light. We found a strong dispersion of the optic axial angle, which decreases from $\approx 90^\circ$ to zero going from the blue to the green range of the optical spectrum.⁸ Now we report about measurements of the indicatrix orientation, optic axial angle, birefringence, and absorption on monomer crystals of DNP done recently in more detail. Observing in the whole visible spectrum (VIS) and near infrared range (NIR) the dispersion turns out to be a rare crossed-axial-plane dispersion.

CRYSTAL STRUCTURE

DNP crystallizes in the monoclinic system: $a = 5.189 \text{ \AA}$, $b = 11.932 \text{ \AA}$, $c = 14.729 \text{ \AA}$, $\beta = 98.56^\circ$; $V = 901.7 \text{ \AA}^3$; $Z = 2$; space group $P2_1/n$ ($T=296 \text{ K}$).^{5,6} The crystals are columnar, mainly (001) or (010) faced. The columnar axis coincides with the a direction.

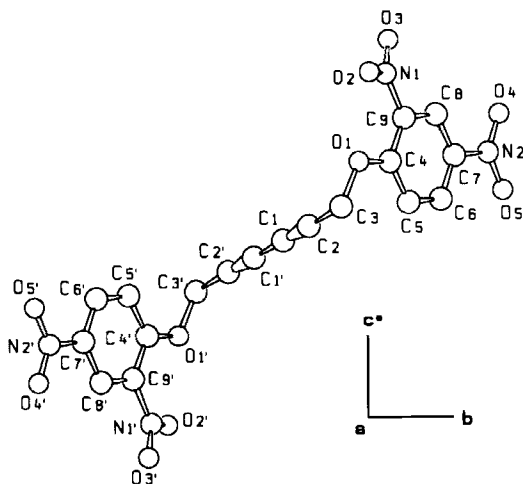


FIGURE 1 View⁹ at the DNP molecule against a direction onto the (b, c^*) plane.

Fig. 1 shows one DNP molecule.⁹ The center of the molecule (between C1 and C1') is inversion point. The stereographic projection (Fig. 2) onto the (001) plane exhibits the orientation of the molecule parts. The ring planes are perpendicular to the plane (001): $\angle ((001), bc) = 89.1^\circ$. The ring planes are strong inclined to the chain direction $(69, 0^\circ)$. The directions of the two NO_2 -groups and of the C4-O1 bond lie in the ring plane. One plane (N2) of the NO_2 -groups coincides with the ring plane. The other group (N1) is inclined to the ring plane by 27.2° .

There exist two intermolecular contacts with distances about equal to the van der Waals distances (Fig. 3). In contact No. 1 H-bonding may be involved.¹⁰

EXPERIMENTAL

Very small crystals were prepared on microscope slides. Measurements were performed by usual polarizing microscope technique using a universal

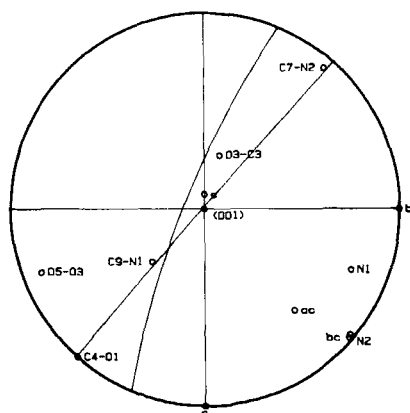


FIGURE 2 Stereographic projection of the DNP molecule related to the (001) plane. ac direction of the acetylene chain. bc normal of the benzene rings. C7 - N2, C9 - N1 directions of the two NO₂-groups. N1, N2 normals of the planes of the two NO₂-groups. C4 - O1 direction of the C-O bond linking ring and chain. O3...C3, O5...O3 directions of distance intermolecular contacts (see Fig. 3).

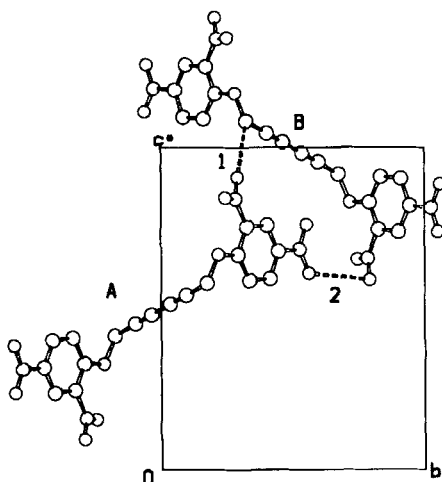


FIGURE 3 View at two DNP molecules against a direction onto the (b, c*) plane. Symmetry operations: A (x, y, z), B (- x + 0.5, y + 0.5, -z + 1.5). Distances of the short intermolecular contacts in A: (1) O3...C3, 2.995 [1.00] and (2) O5...O3, 2.962 [1.06]. Distances in ratio to the van der Waals distances in square brackets.

stage.¹¹ The special equipped microscope (manufactured by Leitz) works in the VIS and NIR from 400 nm to 2000 nm. An additional photometer enables to measure the absorption in the principal directions.

MEASURING RESULTS

The directions of the principal axes of the indicatrix, named optic directions X,Y,Z, are related to the principal diffraction indices (half-axes of the indicatrix) n_α , n_β , n_γ , respectively ($n_\alpha < n_\beta < n_\gamma$). The optic directions coincide with the directions of the principal axes of the polarizability tensor. In monoclinic crystals one optic direction must be coincide with the direction [010] due to the symmetry plane (010).

Indicatrix Orientation

In the range $\tilde{\nu} \gtrsim 2 \cdot 10^4 \text{ cm}^{-1}$ (blue) the optic direction Y parallels b ($Y \parallel b$). Going to lower wavenumbers $\tilde{\nu} \lesssim 1.8 \cdot 10^4 \text{ cm}^{-1}$ (red and NIR) the optic direction X is found parallel to b ($X \parallel b$), i.e. the optic direction Z lying always in the symmetry plane (010). The angle between the a direction and Z is $\angle(a, Z) = 104^\circ$ in obtuse β at $2.2 \cdot 10^4$ and is approximately constant. There is only a little increase by about 5° going from the blue to the red and NIR range.

Optic Axes

The optic direction Z is always acute bisectrix $Z = Bxa$. Fig. 4 shows the dispersion of the axial angle $2V_Z$. In the blue region the optic axial plane coincides with (010). At $\approx 2.2 \cdot 10^4 \text{ cm}^{-1}$ the angle $2V_Z$ is about 80° , i.e. the crystal is nearly optical neutral. The axial angle decreases with decreasing wavenumber. The shape of the indicatrix becomes a long-stretched rotation ellipsoid $n_\gamma \gg n_\beta$, n_α , $n_\beta \approx n_\alpha$. At the transition point $\tilde{\nu}_c \approx 1.9 \cdot 10^4 \text{ cm}^{-1}$ the axial angle is zero, i.e. the crystal is uniaxial (indicatrix is rotation ellipsoid with long axis Z). Below $\tilde{\nu}_c$ the axial angle is about 60° and decreases to a constant value of about 45° by lowering the wavenumber. In the transition region the examination of the indicatrix is impossible. This is also known from other materials (for example mineral Brookite).¹²

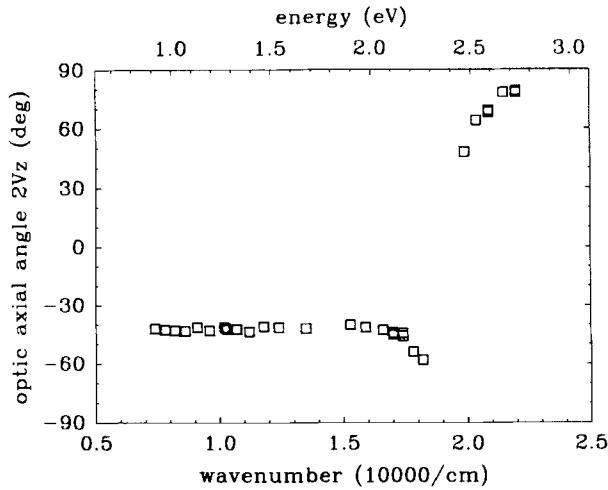


FIGURE 4 Optic axial angle $2V_z$ versus wavenumber. The transition point of the crossed-axial-plane dispersion lies at $\tilde{\nu}_c \approx 1.9 \cdot 10^4 \text{ cm}^{-1}$. In the upper range $\tilde{\nu} > \tilde{\nu}_c$: axial plane $\perp b$, ($Y \parallel b$); in the lower range $\tilde{\nu} < \tilde{\nu}_c$: axial plane $\parallel b$, ($X \parallel b$). For better demonstration (zero crossing) the angles in the lower part are drawn with negative sign.

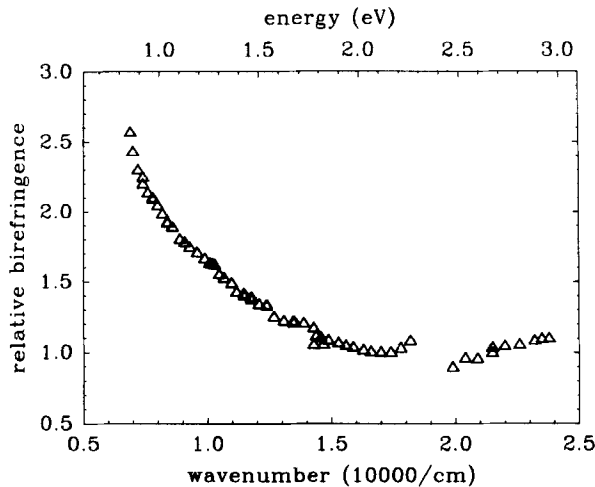


FIGURE 5 Relative birefringence $(n_\beta - n_\alpha)/(n_\beta - n_\alpha)_{\text{NaD}}$ versus wavenumber. $d(n_\beta - n_\alpha)_{\text{NaD}} = 681 \text{ nm}$ retardation measured with NaD-light (589 nm), d effective thickness of the measured crystal sample.

Birefringence

The retardation $\Gamma = d (n_\beta - n_\alpha)$ can be measured looking along Z ($Z = Bxa$). The effective sample thickness d is 6.4% greater than the true thickness due to the sample inclination by $20^\circ = \angle(a, Z) - 90^\circ$. The true sample thickness is unknown. Therefore in Fig. 5 the retardation is plotted related to the retardation measured with NaD-light. Assuming thicknesses between 5 to 10 μm yields values of 0.1 to 0.06 for the birefringence $n_\beta - n_\alpha$ at NaD (Fig. 5).

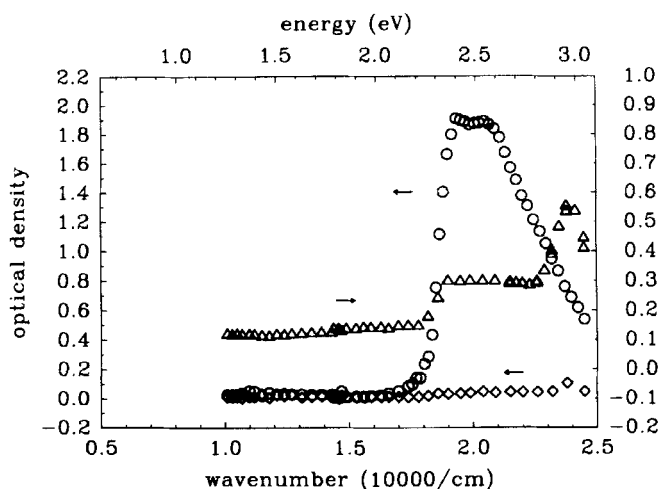


FIGURE 6 Optical density $\log(I_o/I)$ versus wavenumber for polarization parallel to the three optic direction X (o), Y (\diamond), and z (Δ). Two different samples: (X and Y) and (Z).

Absorption

Fig. 6 shows the absorption measured for polarization parallel to the three optic directions X, Y, and Z. To that at least two different oriented crystal samples are needed. The directions of principal axes of the absorption tensor are found coinciding with the optic directions. Light transmitting along Z and polarized parallel X shows a large double peak around 1.93 and $2.05 \cdot 10^4 \text{ cm}^{-1}$. Yellowbrown results for the pleochroism colour. Polarizing parallel to Y yields no considerable absorption. The transmitting light is colourless. Light transmitting along the b direction enables polariza-

tion parallel Z. Plateaulike absorption is found in the double peak region and a single peak at $2.38 \cdot 10^4 \text{ cm}^{-1}$. The pleochroism colour is pale light-orange.

DISCUSSION

For analysing the indicatrix orientation calculations of the polarizabilities were performed.^{13,14} Looking to the molecule structure (Fig.1) the π -electron system can be divided in the two rings and in the acetylene chain due to the strong inclination between the molecule parts (69°).

The tensor \underline{a} of the molar polarizability as calculated by adding up all bond polarizabilities in the rings or in the chain, respectively, $\underline{a} = \sum \underline{a}_j$.¹⁵ Each bond contribution \underline{a}_j was calculated from the orientation and from the polarizability tensor of the bond. Eigenanalysis of \underline{a} yields the principal values of \underline{a} (eigenvalues) and the eigenvectors i.e. the orientation of the polarizability tensor in the crystal coordinate system.¹⁵

In this way calculated polarizabilities for one ring are $\alpha_x = 7.67$ $\alpha_y = 15.91$, $\alpha_z = 17.12$, $\bar{\alpha} = 13.57$ (polarizabilities always in \AA^3). The orientation is drawn in Fig. 7 and approximately coincides with the orientation of the ring (Fig. 7) as was to be expected. The angles are $\angle (N, bc) = 3.6^\circ$ and $\angle (T, (001)) = 3.8^\circ$ i.e. T stands perpendicular to (001). Also the direction of

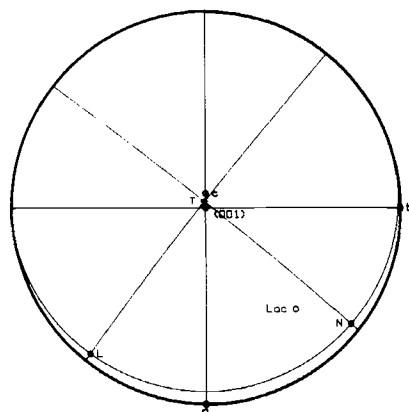


FIGURE 7 Stereographic projection of the orientation of the calculated polarizability tensor (L, T, N) of the rings and direction of the principal polarizability of the acetylene chain Lac. L, T, N directions of the maximum, intermediate, minimum polarizability, respectively. For clarity only one moiety is drawn.

the maximum polarizability of the acetylene chain parallels the chain direction ψ (Lac, ac) = 0.2° with $\alpha = 9.99$ and $\bar{\alpha} = 5.54$.

Superposing the polarizabilities of the different molecule groups to the (010) plane shows (Fig. 7) that the effective polarizability cannot account for the measured extinction angle ψ (a, Z) $\approx 104^\circ$. But it is evident from Fig. 7 that the calculated angle should be $< 90^\circ$, it is 38° . Therefore polarizabilities with other orientations must be involved.

Inspecting the structure points out to the intermolecular contacts (Fig. 2-3). Especially the O3...C3 contact is expected to be dominant. The distance is short (2.995 Å). Also CH...O bridging may be involved.¹⁰ The angle between the a axis and the contact direction is ψ (a, (O3...C3)) = 120.6° . The inclination to the (010) plane is only 8.0° . Assigning polarizability to this contact can explain the measured behavior.^{13,14}

Variation of the polarizability of the intermolecular contact O3...C3 shows that the measured extinction angle ψ (a,Z) = 104° will be reached if the contact polarizability exceeds about 30% of the maximum polarizability of the ring group. This also causes the switching between the two orientations of the axes plane.

The influence of the contact O3...C3 is confirmed by the absorption spectrum. The contact direction stands approximately perpendicular to the b direction (Fig. 1). Therefore no excitation is measured for polarization parallel to the b direction (Fig. 7).

We have shown that the strong dispersion in DNP crystals is governed first of all by the interaction between the polarizability of the benzene ring with its polarizable groups and the polarizability of the intermolecular O3...C3 contact.

Calculations of the molar polarizability (and also of the refractive indices and the axial angle) by going in more detail are in progress and will be published.

ACKNOWLEDGEMENTS

We would like to thank E. Dormann, P. Gruner-Bauer, and I. Müller (Universität Bayreuth) for the crystals and M. Bertault (Université de Rennes) for sending us the atomic coordinates prior to publication.

REFERENCES

1. G. Wegner, Z. Naturforsch., **24b**, 824 (1969).
2. A. R. McGhie, G. F. Lipscomb, A. F. Garito, K. N. Desai, P. S. Kalyanaraman, Makromol. Chem., **182**, 965 (1981).
3. G. F. Lipscomb, A. F. Garito, T. S. Wei, Ferroelectrics, **23**, 161 (1980).
4. H. Schultes, P. Strohhriegl, E. Dormann, Ferroelectrics, **70**, 161 (1986).
5. M. Bertault, L. Toupet, Mater. Sci., **13**, 23 (1987).
6. H. Winter, E. Dormann, M. Bertault, L. Toupet, Phys. Rev., **B 46**, 8057 (1992).
7. M. Dressel, H. W. Helberg, Synth. Metals, **41**, 245 (1991).
8. H. W. Helberg, unpublished (1990).
9. Using program SCHAKAL from E. Keller, Kristallographisches Institut, Universität Freiburg.
10. C. Ramakrishnan, in Computing in Crystallography, edited by R. Diamond, S. Ramaseshan, K. Venkatesan (The Indian Academy of Sciences, Bangalore, 1980) p. 25.11.
11. H. W. Helberg, phys. stat. sol., (a)**33**, 453 (1976).
12. N. H. Hartshorne, A. Stuart, Crystals and the Polarising Microscope, (Edward Arnold, London, 1970), p. 348.
13. H. W. Helberg, H.-Chr. Lenz, Synth. Metals, **56**, 2431 (1993).
14. H. W. Helberg, Physica, **143B**, 488 (1986).
15. S. de Jong, F. Groeneweg, F. van Voorst Vader, J. Appl. Cryst., **24**, 171 (1991).